High-precision relativistic atomic structure calculations and the EBIT

Kwok-Tsang Cheng

Lawrence Livermore National Laboratory

20 Years of Spectroscopy with EBIT

November 13, 2006

This work was performed under the auspices of the U.S. Department of Energy by the University of California Lawrence Livermore National Laboratory under Contract No. W-7405-Eng-48.

Lawrence Livermore National Laboratory, P.O. Box 808, Livermore, CA 94551-0808

UCRL-PRES-225972

Collaborators

Mau-Hsiung Chen, Lawrence Livermore National Laboratory

Walter R. Johnson, University of Notre Dame

Jonathan Sapirstein, University of Notre Dame

Relativistic atomic structure calculations have many important applications

- Tests of strong-field QED in high-*Z* ions
- Tests of PNC and EDM in atoms
- Tests of nuclear effects:
  - Nuclear charge radii and isotope shifts
  - Nuclear magnetization distributions (Bohr-Weisskopf effect)
  - Nuclear recoils and mass polarizations
  - Nuclear polarizations
- Accurate determinations of the fine-structure constant
- Possible time variation of the fine-structure constant
- Diagnostic and modeling of hot, dense plasmas
- Development of x-ray lasers

Relativistic atomic structure calculations

- Multiconfiguration Dirac-Fock (MCDF)
- Relativistic random-phase approximation (RRPA)
- Multiconfiguration relativistic random-phase approximation (MCRRPA)
- Relativistic many-body perturbation theory (RMBPT)
- All-order relativistic coupled-cluster calculations with single-, double-, and partial triple-excitations [CCSD(T)]
- Relativistic configuration-interaction (RCI)

Early tests of QED mostly came from MCDF calculations

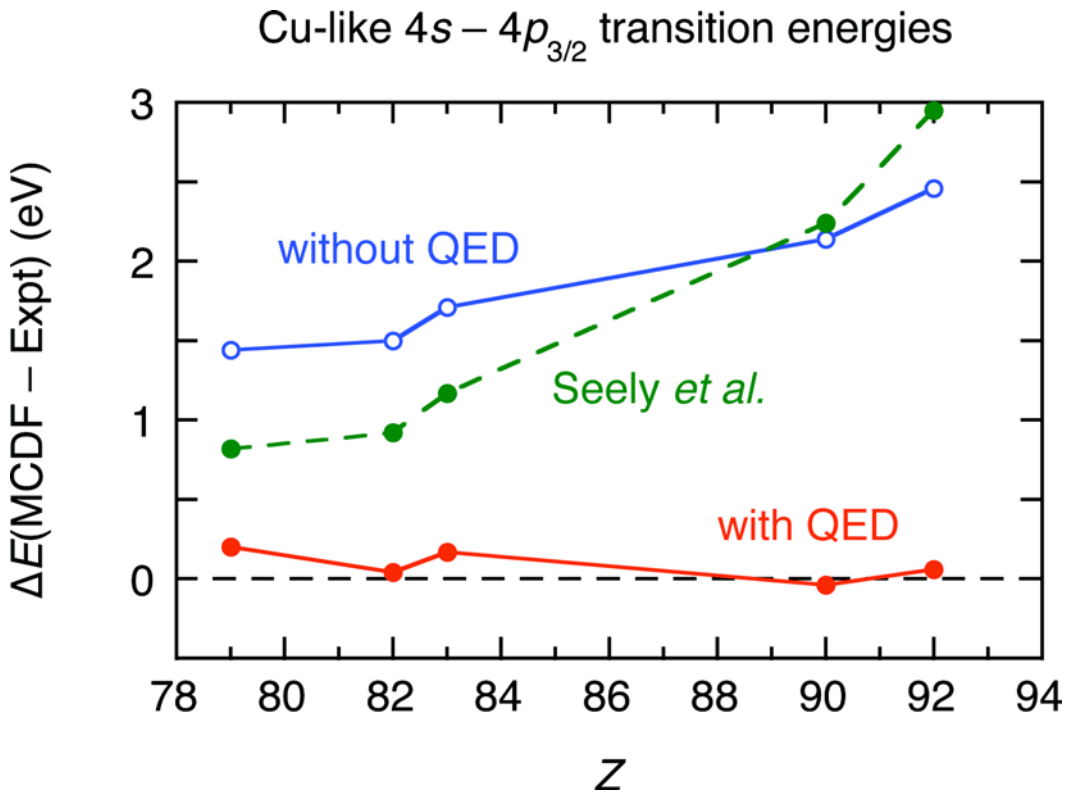

Laser plasma experiment: Seely *et al.*, Phys. Rev. Lett. 57, 2924 (1986)

MCDF theory: Cheng and Wagner, Phys. Rev. A 36, 5435 (1987)

EBIT revealed the limitation of MCDF

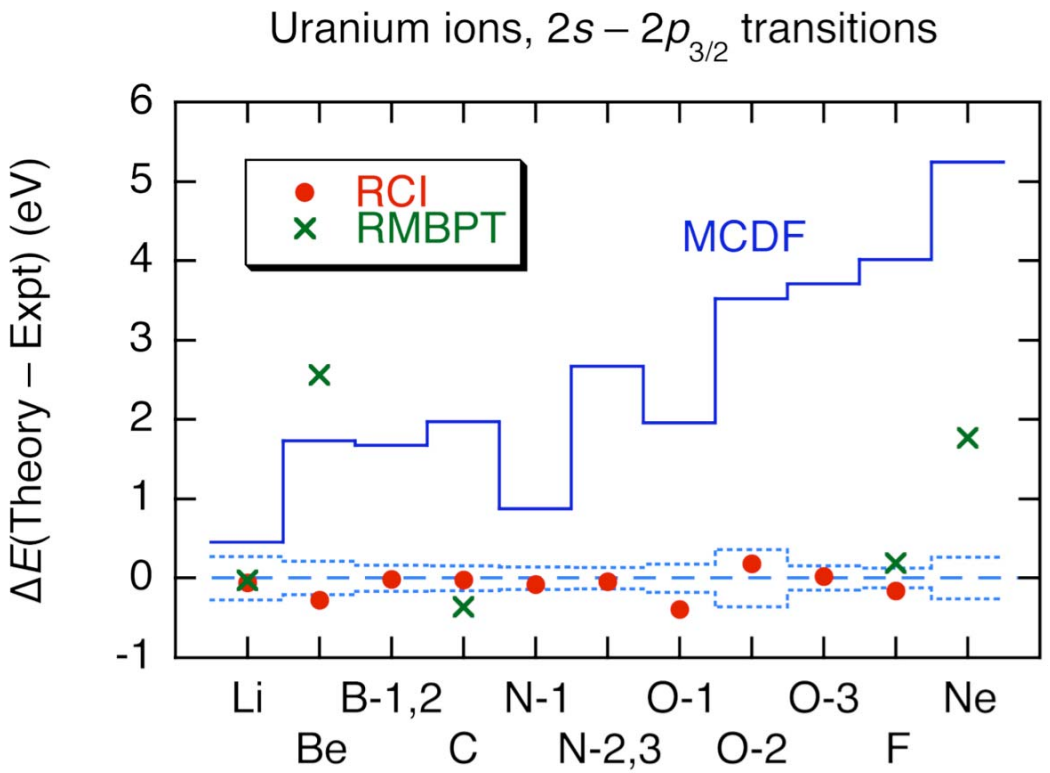

EBIT: Beiersdorfer *et al.*, Phys. Rev. Lett. 71, 3939 (1993)

RMBPT: Johnson *et al.*, Phys. Rev. A 51, 297 (1995)

RCI: Cheng and Chen, Phys. Rev. A 53, 2206 (1996)

Relativistic atomic structure calculations should start from the *no-pair* Hamiltonian

$$H_{\rm no-pair} = \sum_{i=1}^{N} h_i \; + \; \Lambda_{++}\big(H_{\rm C} + H_{\rm B}\big)\Lambda_{++} \; + \sum_{i=1}^{N} \Delta U_i$$

$$h_i = c\vec{\alpha}_i \cdot \vec{p}_i + \beta_i mc^2 + V(r_i) \; ; \qquad \Delta U = V_{\rm nuc}(r_i) - V(r_i)$$

finite nuclear size included

$$H_{\rm C} = \sum_{i>j} \frac{e^2}{r_{ij}}$$

$$H_{\rm B} \quad = \quad -\sum_{i>j} \frac{e^2}{r_{ij}} \left[\vec{\alpha}_i \cdot \vec{\alpha}_j \cos k_0 r_{ij} - (\vec{\alpha}_i \cdot \vec{\nabla}_i)(\vec{\alpha}_j \cdot \vec{\nabla}_j) \frac{\cos k_0 r_{ij} - 1}{k_0^2} \right]$$

$$\xrightarrow[k_0 \to 0]{} -\sum_{i>j} \frac{e^2}{r_{ij}} \left[\vec{\alpha}_i \cdot \vec{\alpha}_j - \frac{\vec{\alpha}_i \cdot \vec{\alpha}_j - (\vec{\alpha}_i \cdot \hat{r}_{ij})(\vec{\alpha}_j \cdot \hat{r}_{ij})}{2} \right]$$

Λ_{++} : positive-energy projection operators ; $k_0 = \omega / c$

Many-electron Dirac Hamiltonian is "sick" with the Brown-Ravenhall disease

$$H = h_1 + h_2 + U_{12} \quad ; \quad h|u\rangle = \epsilon|u\rangle$$

$$v_{abcd} = \langle ab\,|U_{12}|\,cd\rangle \quad ; \quad \tilde{v}_{abab} = v_{abcd} - v_{abdc}$$

$$E = E_0 + E_1 + E_2 + \ldots$$

$$E_0 = \epsilon_a + \epsilon_b$$

$$E_1 = -\frac{1}{2}\sum_{ab} \tilde{v}_{abab}$$

$$E_2 = -\frac{1}{2}\sum_{abmn} \frac{v_{abmn}\tilde{v}_{mnab}}{\epsilon_m + \epsilon_n - \epsilon_a - \epsilon_b}$$

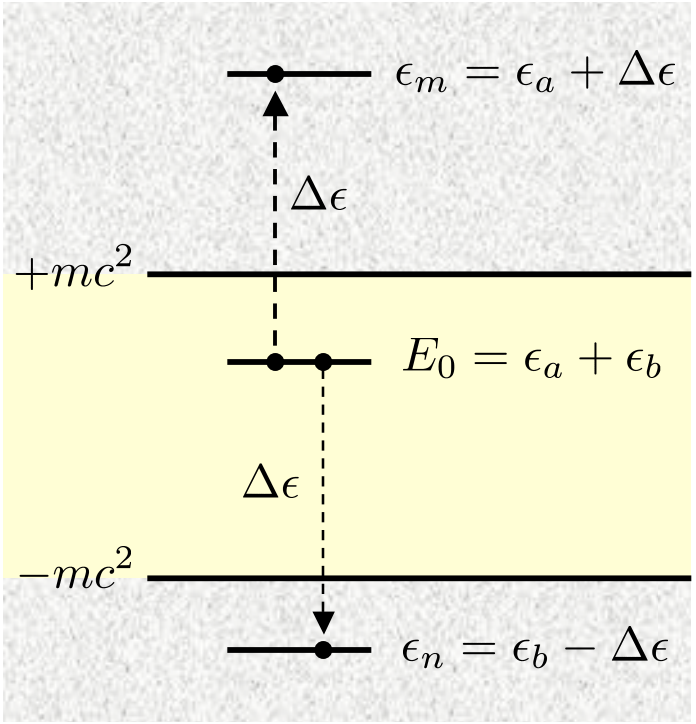

For any negative-energy state $|n_-\rangle$, there will always be a positive-energy state $|m_+\rangle$ such that $|m_+n_-\rangle$ is degenerate in energy with $|ab\rangle$. In effect, all bound states are imbedded in an electron-positron continuum and will "autoionize" (spontaneously decay) into electron-positron pairs.

Second-order energies from the many-electron Dirac Hamiltonian are incorrect

$$E^{(2)}_{\rm Dirac} = -\frac{1}{2}\sum_{abm_+n_+}\frac{v_{abm_+n_+}\tilde{v}_{m_+n_+ab}}{\epsilon_{m_+}+\epsilon_{n_+}-\epsilon_a-\epsilon_b} - \frac{1}{2}\sum_{abm_-n_-}\frac{v_{abm_-n_-}\tilde{v}_{m_-n_-ab}}{\epsilon_{m_-}+\epsilon_{n_-}-\epsilon_a-\epsilon_b}$$
$$-\frac{1}{2}\sum_{abm_+n_-}\frac{v_{abm_+n_-}\tilde{v}_{m_+n_-ab}}{\epsilon_{m_+}+\epsilon_{n_-}-\epsilon_a-\epsilon_b} - \frac{1}{2}\sum_{abm_-n_+}\frac{v_{abm_-n_+}\tilde{v}_{m_-n_+ab}}{\epsilon_{m_-}+\epsilon_{n_+}-\epsilon_a-\epsilon_b}$$

Second-order QED energies from the ladder and cross-ladder diagrams are rigorous and do not suffer from the Brown-Ravenhall disease [Sapirstein *et al.*, Phys. Rev. A 59, 259 (2001)]

$$E^{(2)}_{Ladder} = -\frac{1}{2}\sum_{abm_+n_+}\frac{v_{abm_+n_+}\tilde{v}_{m_+n_+ab}}{\epsilon_{m_+}+\epsilon_{n_+}-\epsilon_a-\epsilon_b} + \frac{1}{2}\sum_{abm_-n_-}\frac{v_{abm_-n_-}\tilde{v}_{m_-n_-ab}}{\epsilon_{m_-}+\epsilon_{n_-}-\epsilon_a-\epsilon_b}$$

$$E^{(2)}_{xLadder} = -\frac{1}{2}\sum_{abm_+n_-}\frac{v_{an_-m_+b}\,v_{bm_+n_-a}-v_{an_-m_+a}\,v_{bm_+n_-b}}{\epsilon_{n_-}-\epsilon_{m_+}}$$
$$-\frac{1}{2}\sum_{abm_-n_+}\frac{v_{an_+m_-b}\,v_{bm_-n_+a}-v_{an_+m_-a}\,v_{bm_-n_+b}}{\epsilon_{m_-}-\epsilon_{n_+}}$$

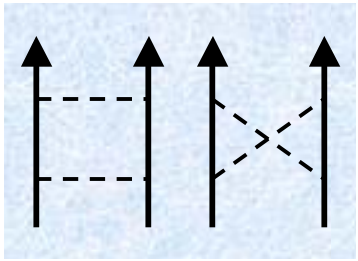

No-pair energies are potential and gauge dependent

Second-order energies of the $1s^2$ ground state of He-like uranium

E(eV)	Potential	$E_{\text{no-pair}}$	E_{Dirac}	ΔE_{Dirac}	E_{QED}	ΔE_{QED}
Coul	Coul	-262235.48	-262235.10	0.38	-262235.18	0.30
	DKS	-262235.42	-262235.10	0.32	-262235.18	0.24
	ΔE	-0.06	0.00		0.00	
Breit	Coul	327.29	333.74	6.45		
	DKS	327.10	333.74	6.64		
	ΔE	0.19	0.00			

Sapirstein *et al.*, Phys. Rev. A 59, 259 (2001)

- E_{Dirac} , though potential independent, are different from E_{QED} from the ladder and cross-ladder diagrams
- ΔE_{Dirac} and ΔE_{QED} are contributions from negative-energy states and can be sizable for Breit energies

He-like uranium RCI energies calculated with and without negative-energy basis functions

The spectra of E_{Dirac} in cavities with radii $R = 0.8$ and 1.2 a.u. show cavity-dependent spurious states which are essentially *discrete representations* of the *unphysical* electron-positron continuum

State	$E_{no\text{-}pair}(R = 0.8 \text{ \& } 1.2)$	$E_{Dirac}(R = 0.8)$	$E_{Dirac}(R = 1.2)$
$1s2s\ ^1S_0$	-6081.587	-6081.584	-6081.584
		⋮	⋮
		⋮	-8971.861
		-8858.069	-9061.937
		-8866.694	-9405.122
		-9064.952	-9424.240
$1s^2\ ^1S_0$	-9636.993	-9636.979	-9636.979
		-9658.276	-9661.932
		-10463.597	-9752.548
		⋮	-10009.984
		⋮	⋮

Sapirstein *et al.*, Phys. Rev. A 59, 259 (2001)

B-spline, or basis spline, functions of order *k* are piecewise polynomials of degree *k* - 1

B-spline functions $\{B_{i,k}(r),\ i = 1, 2, \ldots, n\}$ with $k = 6$ and $n = 30$ covering an interval 0 to 40 a.u. divided into an "atomic grid"

Atomic orbitals can be expanded in terms of $\{B_{i,k}(r),\ i = 1, 2, \ldots, n\}$ which form a complete basis set. The dotted curve in the following figure is the large component of the $Z = 2$ Coulomb $2s$ wave function

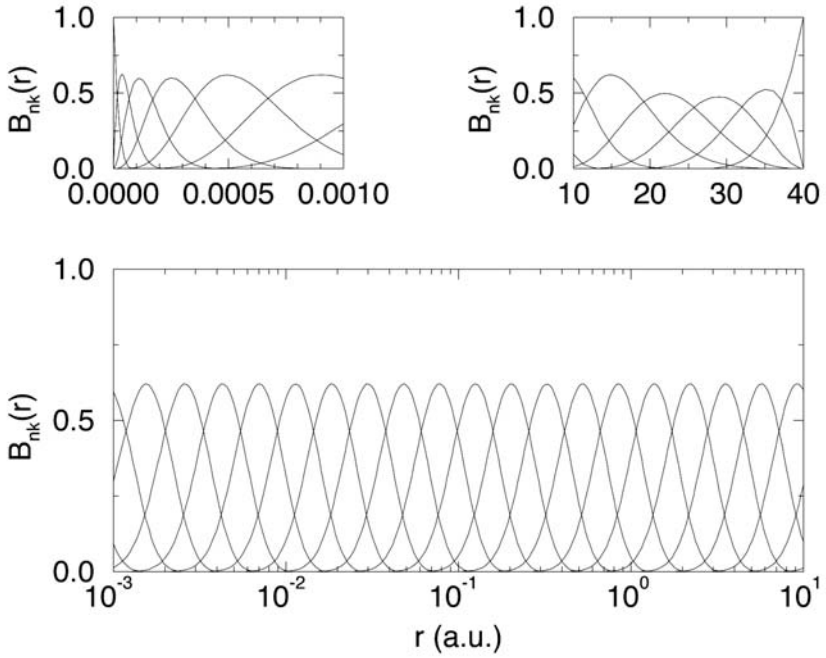

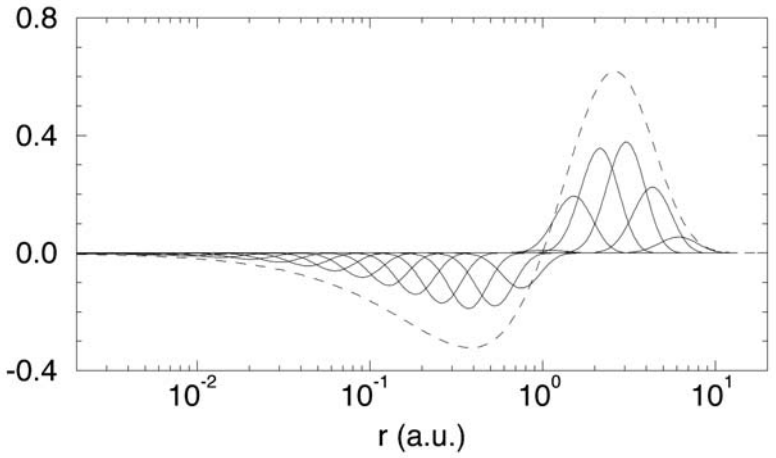

One-electron *B*-spline basis functions

- One-electron *B*-spline basis functions are Dirac orbitals of an electron confined in a cavity and subjected to boundary conditions imposed by the MIT bag model [Johnson *et al.*, Phys. Rev. A 37, 307 (1988)]
- *B*-spline orbitals are discrete, finite, and cleanly separates into *n* positive- and *n* negative-energy states. By using only positive-energy basis functions in atomic structure calculations, the no-pair requirement is implicitly satisfied
- *B*-spline orbitals form a complete basis set as verified by sum rule calculations and are suitable for RMBPT and QED calculations involving sums over intermediate states

RCI calculations with *B*-spline basis sets

- There are no spurious states in the spectrum of *B*-spline orbitals and no variational collapse problems in RCI calculations using these basis functions
- Typically, 30 to 40 positive-energy *B*-spline orbitals of orders 7 to 9 are generated for each angular symmetries s, $p_{1/2}$, $p_{3/2}$, $d_{3/2}$ … and the first 20 to 25 orbitals are used
- Resulting basis sets are big and lead to large-scale RCI expansions which have reached close to 1/2 million configurations
- Davidson's method as implemented by Stathopoulos and Fischer [Comput. Phys. Comm. 79, 268 (1994)] is used to solve for the first few eigenstates of huge RCI matrices
- Correlation contributions from bound and continuum states can be *systematically* included for well converged RCI results

Typical configuration expansions in RCI calculations

Ion	Reference state	Single & double excitations		Triple excitations
Li-like	$1s^2 2s$	CV	$1s n\ell n'\ell'$	$2p n\ell n'\ell'$, $3s n\ell n'\ell'$
		CC	$2s n\ell n'\ell'$	…
	$1s^2 2p$	CV	$1s n\ell n'\ell'$	$2s n\ell n'\ell'$, $3s n\ell n'\ell'$
		CC	$2p n\ell n'\ell'$	…
Be-like	$1s^2 2s^2 + 1s^2 2p^2$	VV	$1s^2 n\ell n'\ell'$	$2s2p n\ell n'\ell'$
		CV	$1s2s n\ell n'\ell'$, $1s2p n\ell n'\ell'$	$2s3s n\ell n'\ell'$, $2p3s n\ell n'\ell'$
		CC	$2s^2 n\ell n'\ell'$, $2p^2 n\ell n'\ell'$	…
	$1s^2 2s2p$	VV	$1s^2 n\ell n'\ell'$	$2s^2 n\ell n'\ell'$, $2p^2 n\ell n'\ell'$
		CV	$1s2s n\ell n'\ell'$, $1s2p n\ell n'\ell'$	$2s3s n\ell n'\ell'$, $2p3s n\ell n'\ell'$
		CC	$2s2p n\ell n'\ell'$	…

Theory and experiment agree for the transition energies (eV) of low- to mid-*Z* Li-like ions

Ion	Ne^{7+}	P^{12+}	Ca^{17+}	Fe^{23+}	Ge^{29+}	Mo^{39+}	Xe^{51+}
			$2s - 2p_{1/2}$				
RMBPT	15.8885	25.812	35.964	48.602	61.911	86.12	119.84
RCI	15.8888	25.813	35.963	48.600	61.907	86.11	119.82
Expt	15.8887(2)	25.814(3)	35.962(2)	48.599(1)	61.902(4)	86.10(1)	119.97(10)
			$2s - 2p_{3/2}$				
RMBPT	16.0931	27.205	41.028	64.568	101.055	211.99	492.22
RCI	16.0933	27.205	41.028	64.567	101.051	211.99	492.21
Expt	16.0932(2)	27.206(3)	41.029(2)	64.566(2)	101.043(12)	211.94(7)	492.34(62)

Chen *et al.*, Phys. Rev. A 52, 266 (1995)

Li-like $2s$ - $2p_{1/2}$ transition energies relative to RCI energies are scaled by Z^2

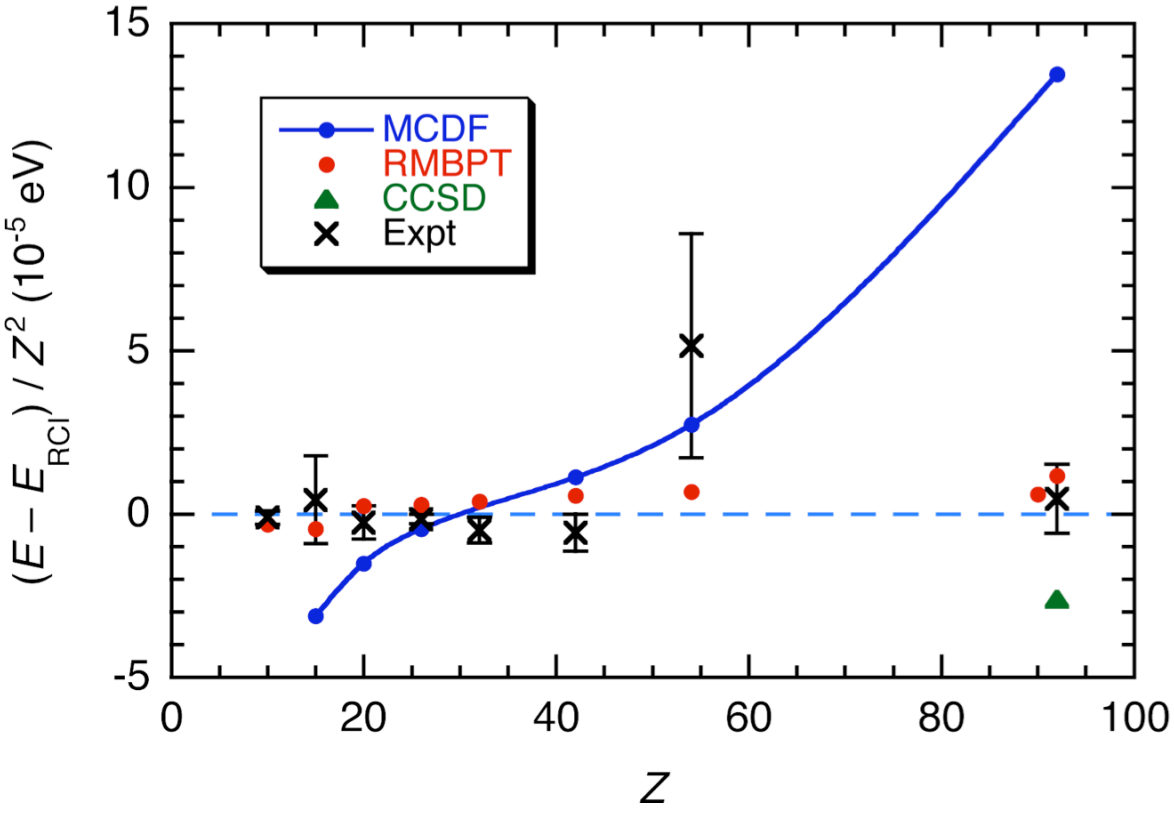

Chen *et al.*, Phys. Rev. A 52, 266 (1995)

Be-like $2s^2\ ^1S_0$ - $2s2p\ ^1P_1$ transition energies relative to RCI energies are scaled by Z

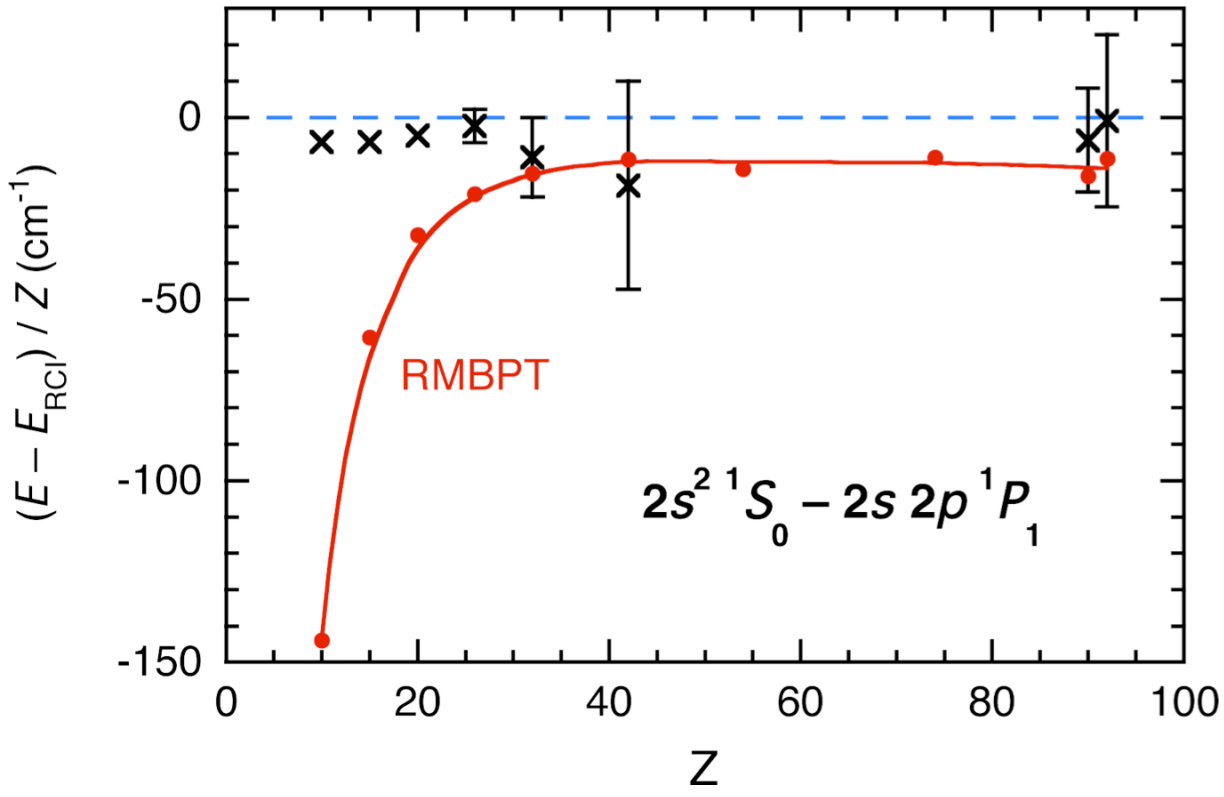

RCI: Chen and Cheng, Phys. Rev. A 55, 166 (1997)
RMBPT: Safronova *et al.*, Phys. Rev. A 53, 4036 (1996)

RCI and RMBPT energies for uranium ions

	Li-like $2s$ - $2p_{1/2}$			Li-like $2s$ - $2p_{3/2}$			Be-like $^1S_0$ - $^1P_1$		
	RCI[a]	RMBPT[b]		RCI[a]	RMBPT[b]		RCI[c]	RMBPT[d]	
Coul	286.12	286.14		4514.79	4514.81				
Breit	36.10	36.27	*0.17*	-15.88	-16.21	*-0.33*			
MP	-0.05	-0.03		-0.04	-0.04				
Structure	322.17	322.38	*0.21*	4498.87	4498.56	*-0.31*	4539.89	4539.49	*-0.40*
QED	-41.62	-41.68	*-0.06*	-39.69	-39.13	*0.56*	-38.48	-37.89	*0.59*
Theory	280.55	280.70	*0.15*	4459.18	4459.43	*0.25*	4501.41	4501.60	*0.19*
EBIT	280.645(15)[e]			4459.37(21)[f]			4501.72(27)[f]		
QED-deduced	-41.53	-41.74	*-0.21*	-39.50	-39.19	*0.31*	-38.17	-37.77	*0.40*

[a]Chen *et al.*, Phys. Rev. A 52, 266 (1995)
[b]Blundell, Phys. Rev. A 47, 1790 (1993)
[c]Chen and Cheng, Phys. Rev. A 55, 166 (1997)
[d]Safronova *et al.*, Phys. Rev. A 53, 4036 (1996)
[e]Beiersdorfer *et al.*, Phys. Rev. Lett. 95, 233003 (2005)
[f] Beiersdorfer *et al.*, Phys. Rev. Lett. 71, 3939 (1993)

Scaled QED energies for the $2s$ - $2p_{3/2}$ transition in Li-like ions

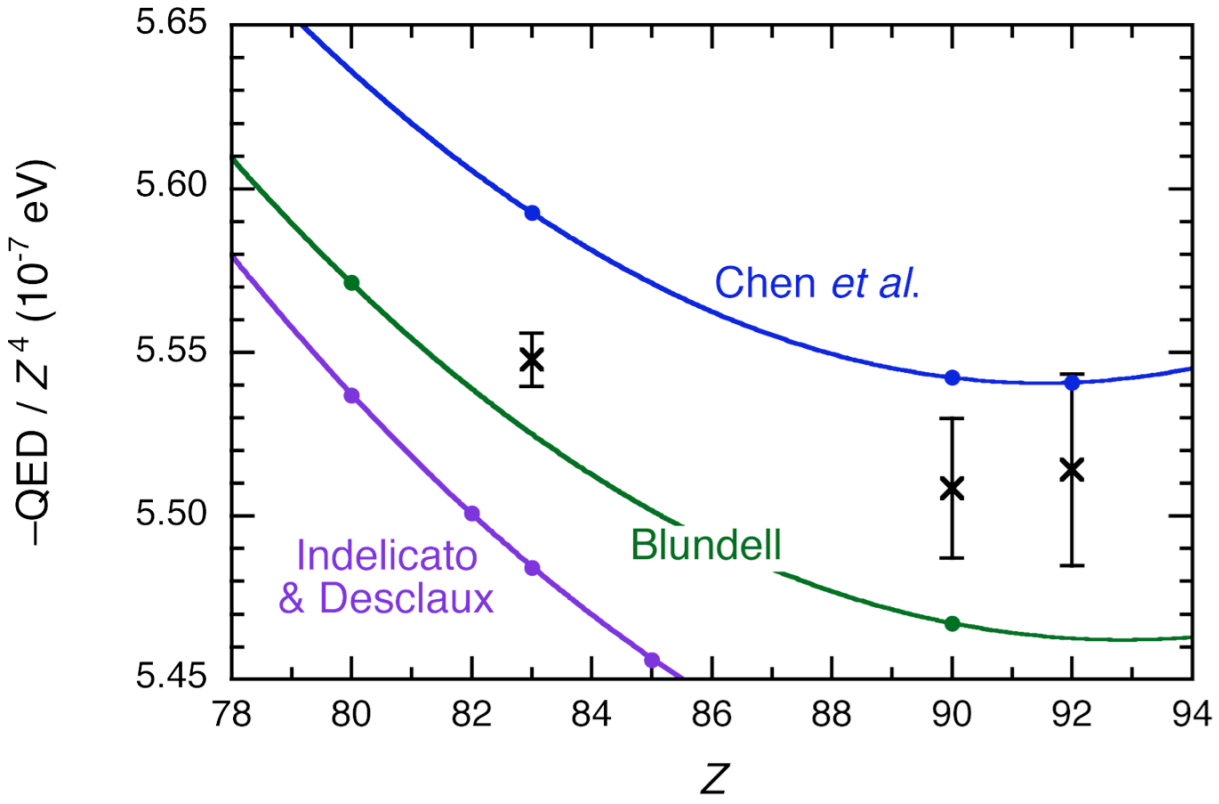

EBIT: Beiersdorfer *et al.*, Phys. Rev. Lett. 80, 3022 (1998)

Typical correlated QED diagrams

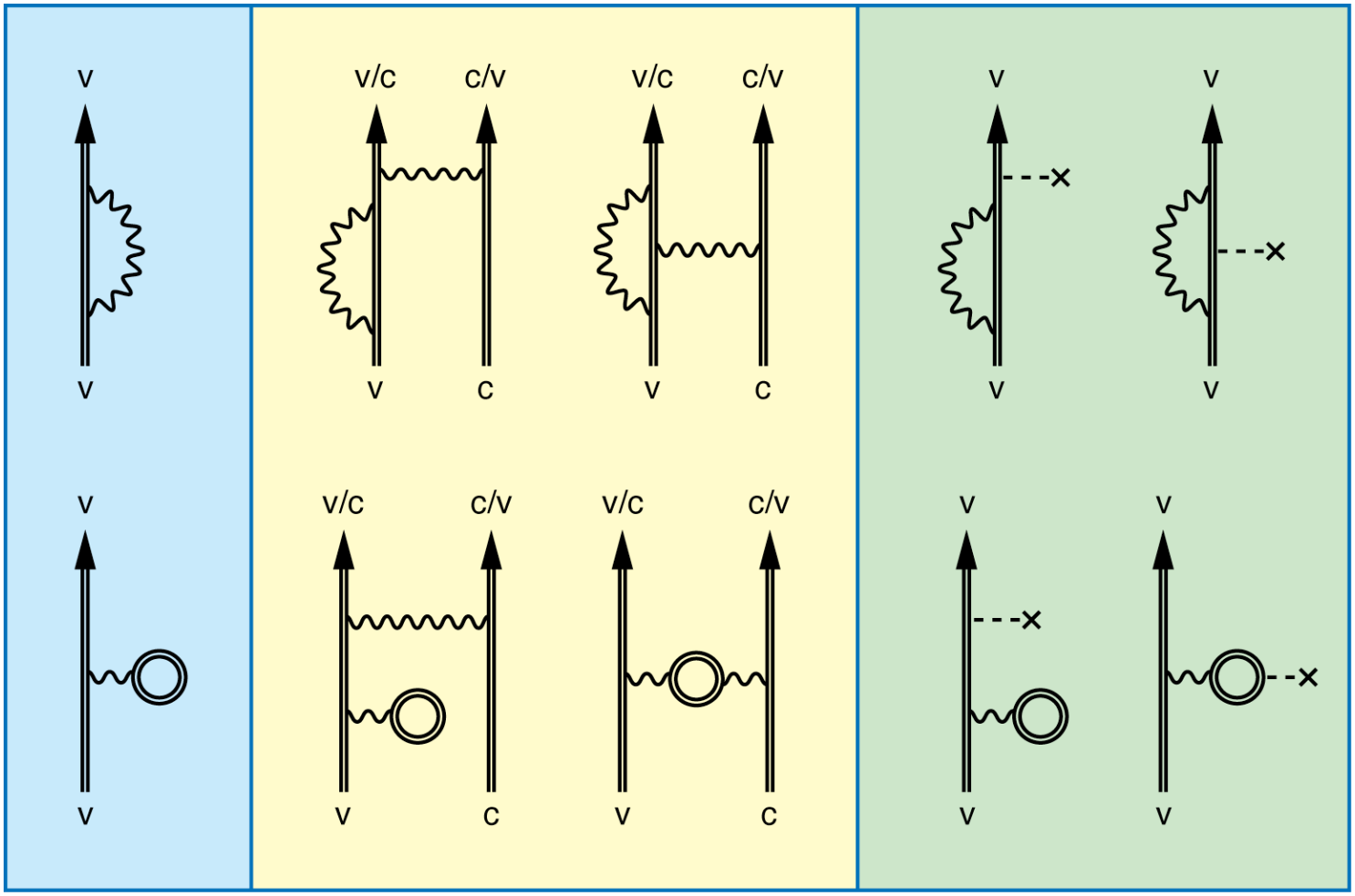

Blundell's treatment of correlated QED diagrams

- 1st-order 1-loop self-energy and vacuum polarization diagrams for the valence and core electrons were calculated with (*N*-1)-electron core-Hartree (CH) and modified core-Hartree (MCH) potentials, respectively

$$V(r) = V_{\rm nuc}(r) + e^2 \int_0^r dr' \frac{1}{r_>} \rho(r')$$

$$\rho_{\rm CH}(r) = \sum_c (2j_c + 1)\rho_c(r) \; ; \quad \rho_{\rm MCH}(r) = \rho_v(r) + \sum_c{}' (2j_c + 1)\rho_c(r)$$

- 2nd-order direct-interaction diagrams were cancelled exactly by the counter-potential diagrams with the use of CH and MCH potentials
- 2nd-order exchange-interaction "side" diagrams were calculated as 1-loop diagrams with perturbed orbitals
- 2nd-order exchange-interaction "vertex" diagrams were left uncalculated

Frozen-core and relax-core QED calculations

- ***N*-electron Kohn-Sham (KS) potentials were used to evaluate 1-loop diagrams:**

$$V(r) \rightarrow V(r) + V_{\rm ex} = -x_\alpha \frac{e^2}{r} \left[\frac{81}{32\pi^2} r\,\rho(r)\right]^{1/3}$$

$$\rho(r) = \rho_v(r) + \sum_c (2j_c + 1)\rho_c(r)$$

- ε_{1s} , ε_{2s} **and** ε_{2p} **are QED energies from the** $1s^2 2s$ **KS potential**
- ε'_{1s} , ε'_{2s} **and** ε'_{2p} **are QED energies from the** $1s^2 2p$ **KS potential**
- **Frozen-core approximation includes only valence contributions:**

$$\Delta\varepsilon_{\rm v} = \varepsilon'_{2p} - \varepsilon_{2s} \approx \varepsilon_{2p} - \varepsilon_{2s}$$

- **Relax-core approximation adds core contributions:**

$$\Delta\varepsilon_{\rm c} = 2\varepsilon'_{1s} - 2\varepsilon_{1s}$$

QED relax-core results are in good agreement with EBIT measurements

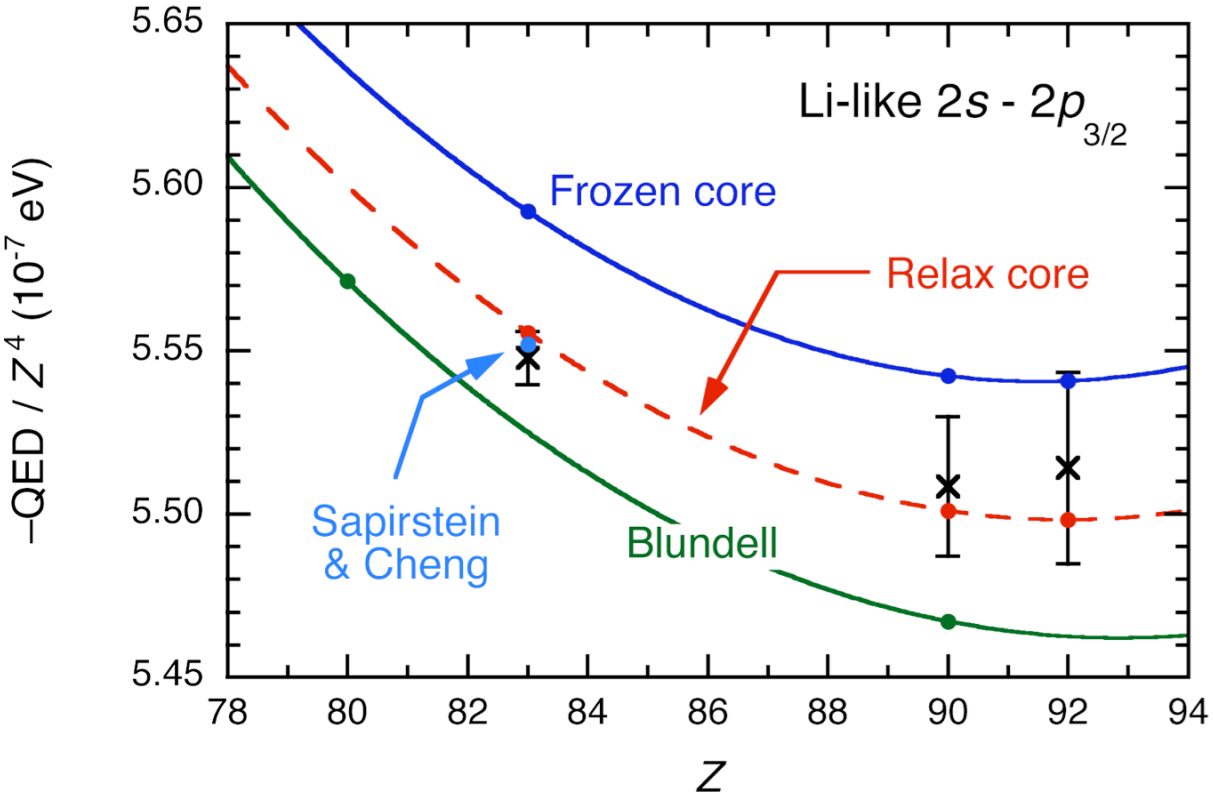

Frozen- and relax-core QED: Cheng *et al.*, Phys. Rev. A 62, 054501 (2000)

Sapirstein and Cheng: Phys. Rev. A 64, 022502 (2001)

Two-loop Lamb shifts and negative-energy states (NES) contributions

	Li-like Bi^{80+} $2s - 2p_{3/2}$		Li-like U^{89+} $2s - 2p_{1/2}$	
	RCI[a]	*S*-matrix[b]	RCI[a]	*S*-matrix[b]
Structure	2814.47	2814.312	322.17	322.21
QED	-26.37	-26.348	-41.72	-41.77
Sum	2788.10	2787.964	280.45	280.44
2-loop	0.175		0.205	
NES	-0.16		0.04	
Theory	2788.115		280.695	
EBIT	2788.139 ± 0.039[c]		280.645 ± 0.015[d]	

[a] Cheng *et al.*, Phys. Rev. A 62, 054501 (2000)
[b] Sapirstein and Cheng: Phys. Rev. A 64, 022502 (2001)
[c] Beiersdorfer *et al.*, Phys. Rev. Lett. 80, 3022 (1998)
[d] Beiersdorfer *et al.*, Phys. Rev. Lett. 95, 233003 (2005)

Other small corrections

- **Nuclear polarization: +0.03 eV for Li-like U^{89+} $2s$ - $2p$ transitions [Plunien and Soff, Phys. Rev. A 51, 1119 (1995); 53, 4614 (1996)]**
- **Nuclear recoils [Artemyev *et al.*, Phys. Rev. A 52, 1884 (1995)]**
  - **Mass polarization (Coulomb photon-exchange only): -0.08 eV**

$$\frac{1}{M}\sum_{i>j}\vec{p}_i\cdot\vec{p}_j$$

  - **One transverse-photon exchange: +0.06 eV —> -0.02 eV**

$$\frac{1}{M}\sum_{i>j}\left(-\frac{Z\alpha}{r_i}\right)\left[\vec{\alpha}_i+\frac{(\vec{\alpha}_i\cdot\vec{r}_i)\vec{r}_i}{r_i^2}\right]\cdot\vec{p}_j$$

  - **Two transverse-photon exchange: -0.05 eV —> -0.07 eV**
  - **MP as calculated:** $(\vec{p}\rightarrow mc\vec{\alpha}\ ;\ \ \vec{p}_i\cdot\vec{p}_j\rightarrow\vec{\alpha}_i\cdot\vec{\alpha}_j\ )$ **-0.04 eV**
  - **Residual nuclear recoil correction: -0.03 eV**

Mg-like ions $3s^2\ {}^1S_0$ - $3s3p\ {}^1P_1$ transition energy

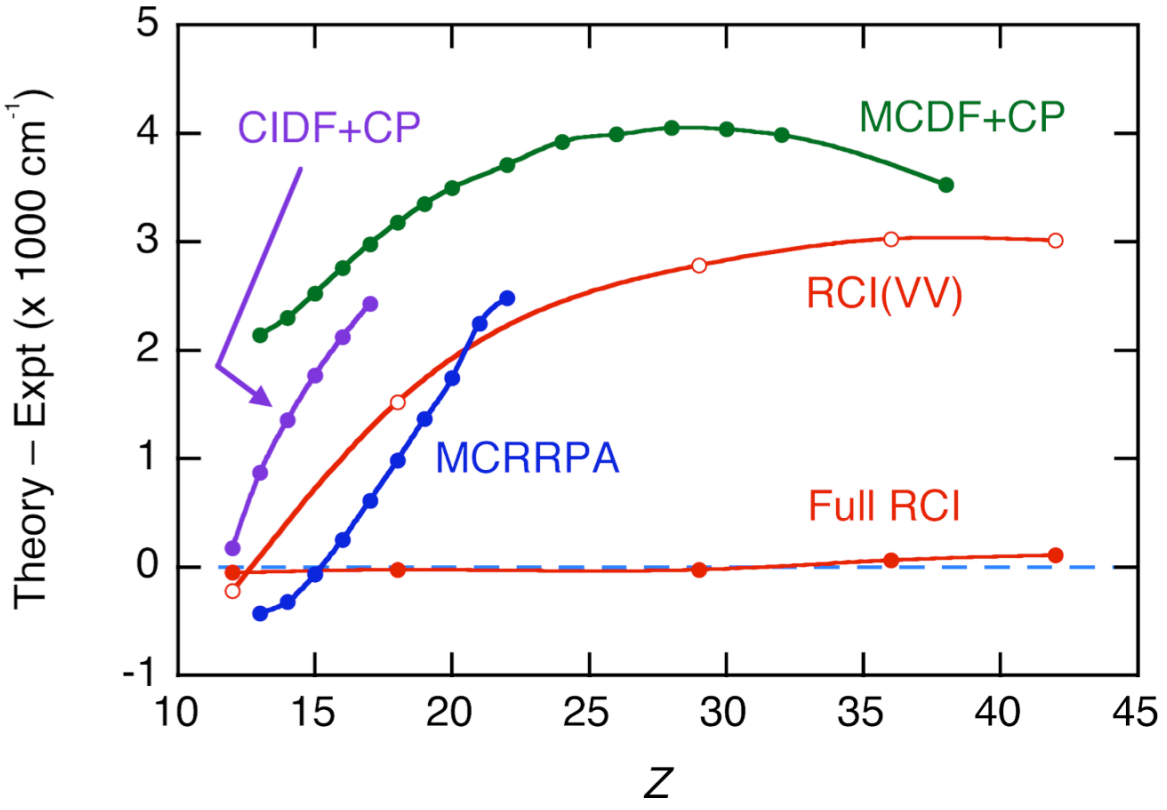

Chen and Cheng, Phys. Rev. A 55, 3440 (1997)

$3s$ - $3p_{3/2}$ transition energies (eV) in Na-like to Si-like uranium

		Na-1	Mg-1	Al-1	Al-2	Si-1
RCI	Coul	1318.14	1329.48	1332.25	1316.00	1319.02
	Breit	-2.79	-2.75	-2.29	-5.99	-5.57
	MP	-0.01	-0.01	-0.01	-0.01	-0.01
	Sum	1315.34(2)	1326.72(2)	1329.95(2)	1310.00(7)	1313.44(7)
QED	SE	-14.21	-13.99	-13.98	-10.39	-10.59
	Uehling	4.10	4.04	4.03	2.98	3.04
	WK	-0.20	-0.20	-0.20	-0.15	-0.15
	Relax	0.08	0.08	0.08	0.14	0.13
	Sum	-10.23(7)	-10.07(7)	-10.07(7)	-7.42(7)	-7.57(7)
Theory		1305.11(7)	1316.65(7)	1319.88(7)	1302.58(10)	1305.87(10)
EBIT		1305.12(2)	1316.64(1)	1319.86(2)	1302.55(2)	1305.76(2)

Chen *et al.*, Phys. Rev. A 68, 022507 (2003)

4*s* - 4*p* and 4*p* - 4*d* transition energies in high-*Z* Cu-like ions

Z	RCI	QED				Theory	EBIT	Laser
	RMBPT	frozen	Δrelax	2-loop	Total			Plasma
				$4s - 4p_{3/2}$				
74	200.13	-1.25	0.01	0.00	-1.24	198.89	198.90(1)	198.99(5)
79	255.01	-1.65	0.01	0.01	-1.63	253.38	253.40(1)	253.40(8)
82	294.45	-1.93	0.01	0.01	-1.91	292.55	292.59(4)	292.65(10)
90	430.03	-2.86	0.02	0.02	-2.82	427.21	427.20(1)	427.68(22)
92	472.30	-3.14	0.03	0.02	-3.09	469.21	469.22(3)	469.53(25)
				$4p_{1/2} - 4d_{3/2}$				
83	367.21	-0.31	0.05	0.00	-0.27	366.94	366.97(2)	
90	492.42	-0.56	0.07	0.00	-0.49	491.93	491.94(10)	
92	535.69	-0.66	0.08	0.00	-0.58	535.11	535.15(5)	

Chen *et al.*, Phys. Rev. A 74, 042510 (2006)

Scaled QED energies (eV) of the $4p_{1/2}$ - $4d_{3/2}$ transition in high-Z Cu-like ions

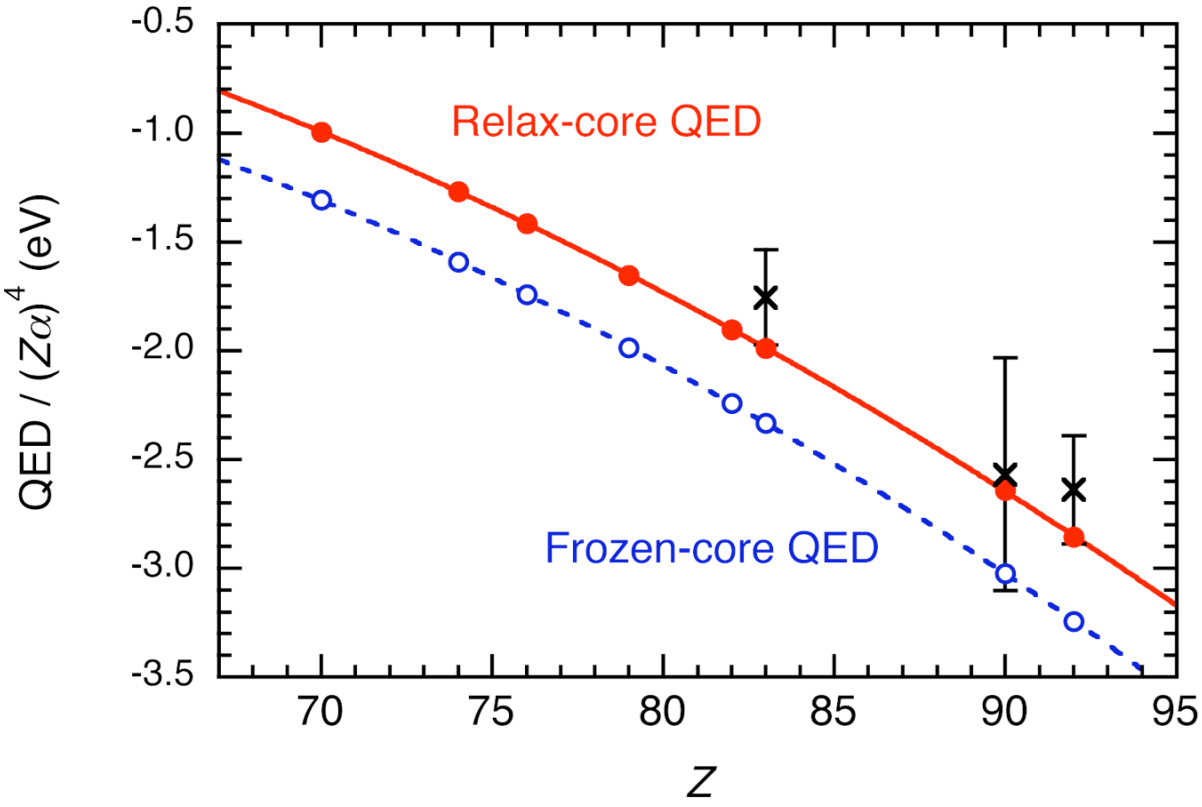

Chen *et al.*, Phys. Rev. A 74, 042510 (2006)

Summary

- EBIT has provided stringent tests of relativistic atomic structure and QED theories
- Advances in theory and experiment make possible tests of ever smaller effects
- We look forward to new EBIT measurements to challenge theory in years to come